

FIRST DETECTION OF HCO⁺ EMISSION AT HIGH REDSHIFTDOMINIK A. RIECHERS¹, FABIAN WALTER¹, CHRISTOPHER L. CARILLI², AXEL WEISS³,
FRANK BERTOLDI⁴, KARL M. MENTEN³, KIRSTEN K. KNUDSEN¹, AND PIERRE COX⁵*draft version October 16, 2018, accepted for publication in the Astrophysical Journal Letters*

ABSTRACT

We report the detection of HCO^{+(J=1→0)} emission towards the Cloverleaf quasar ($z = 2.56$) through observations with the Very Large Array. This is the first detection of ionized molecular gas emission at high redshift ($z > 2$). HCO⁺ emission is a star formation indicator similar to HCN, tracing dense molecular hydrogen gas ($n(\text{H}_2) \simeq 10^5 \text{ cm}^{-3}$) within star-forming molecular clouds. We derive a lensing-corrected HCO⁺ line luminosity of $L'_{\text{HCO}^+} = 3.5 \times 10^9 \text{ K km s}^{-1}\text{pc}^2$. Combining our new results with CO and HCN measurements from the literature, we find a HCO⁺/CO luminosity ratio of 0.08 and a HCO⁺/HCN luminosity ratio of 0.8. These ratios fall within the scatter of the same relationships found for low- z star-forming galaxies. However, a HCO⁺/HCN luminosity ratio close to unity would not be expected for the Cloverleaf if the recently suggested relation between this ratio and the far-infrared luminosity were to hold. We conclude that a ratio between HCO⁺ and HCN luminosity close to 1 is likely due to the fact that the emission from both lines is optically thick and thermalized and emerges from dense regions of similar volumes. The CO, HCN and HCO⁺ luminosities suggest that the Cloverleaf is a composite AGN-starburst system, in agreement with the previous finding that about 20% of the total infrared luminosity in this system results from dust heated by star formation rather than heating by the AGN. We conclude that HCO⁺ is potentially a good tracer for dense molecular gas at high redshift.

Subject headings: galaxies: active, starburst, formation, high redshift — cosmology: observations — radio lines: galaxies

1. INTRODUCTION

One important goal in studies of galaxy formation is to determine star formation characteristics through observations of molecular gas in the early universe. Molecular gas in high-redshift galaxies is commonly traced by CO emission and has been found in >30 galaxies at $z > 2$ to date. The observed molecular gas with masses of $\geq 10^{10} \text{ M}_\odot$ provides the requisite material for star formation (see review by Solomon & Vanden Bout 2005, and references therein).

CO is a good indicator for the total molecular gas content of a system, as it can be excited at relatively low densities; its low dipole moment of $\mu_{\text{D}}^{\text{CO}} = 0.1$ implies a critical density of only $n_{\text{H}_2} \sim 10^2 - 10^3 \text{ cm}^{-3}$ for the lower- J transitions. Hence, emission from low- J CO transitions is a relatively poor tracer of the denser gas that is more intimately associated with star formation. The most common tracers of the dense molecular gas phase are HCN and HCO⁺. Both molecules have much higher dipole moments ($\mu_{\text{D}}^{\text{HCN}} = 2.98$, $\mu_{\text{D}}^{\text{HCO}^+} = 4.48$) than CO. The critical density to collisionally thermalize their lower- J transitions is therefore much higher than for CO, $n_{\text{H}_2} \sim 10^5 - 10^6 \text{ cm}^{-3}$ (e.g. Gao & Solomon

2004a, 2004b; Brouillet et al. 2005).

Recent studies of the dense molecular gas phase in nearby ($z < 0.3$) luminous and ultra-luminous infrared galaxies (LIRGs/ULIRGs) have shown that the HCN and HCO⁺ luminosities correlate with the star-formation rate as traced by the far-infrared (FIR) luminosity. These correlations are tighter than the correlation between the CO and FIR luminosities (Solomon et al. 1992a; Gao & Solomon 2004a, 2004b; Graciá-Carpio et al. 2006). Due to the relative faintness of the emission lines, HCN has only been detected in four objects at high z to date, and all detections are in the host galaxies of quasars (Solomon et al. 2003; Vanden Bout et al. 2004; Carilli et al. 2005; Wagg et al. 2005).

It has recently been argued that AGN-dominated galaxies have higher HCN/HCO⁺ and HCN/CO luminosity ratios than starburst-dominated galaxies (Kohno et al. 2001; Kohno 2005; Imanishi et al. 2006). In this context, it has been suggested that the presence of X-ray emission emerging from a dust-enshrouded AGN may significantly enhance the chemical abundance of HCN relative to HCO⁺ (Lepp & Dalgarno 1996; Kohno et al. 2001; Usero et al. 2004). Also, the excitation of the HCN molecule may be affected by IR-pumping through a $14 \mu\text{m}$ vibrational band (Aalto et al. 1995). Based on these considerations and their HCO⁺ survey of low- z (U)LIRGs, Graciá-Carpio et al. (2006) suggest that the HCO⁺-to-HCN intensity ratio towards FIR-bright ($L_{\text{FIR}} > 10^{12} \text{ L}_\odot$) objects (like the Cloverleaf) are likely low. Measurements of HCO⁺ emission in high redshift objects would thus lead to new constraints on their dense interstellar medium and, potentially, on the radiation field pervading it.

In this letter, we report the first high- z detection of

¹ Max-Planck-Institut für Astronomie, Königstuhl 17, Heidelberg, D-69117, Germany

² National Radio Astronomy Observatory, PO Box O, Socorro, NM 87801, USA

³ Max-Planck-Institut für Radioastronomie, Auf dem Hügel 69, Bonn, D-53121, Germany

⁴ Argelander-Institut für Astronomie, Universität Bonn, Auf dem Hügel 71, Bonn, D-53121, Germany

⁵ Institut de RadioAstronomie Millimétrique, 300 Rue de la Piscine, Domaine Universitaire, 38406 Saint Martin d'Héres, France

Electronic address: riechers@mpia.de

$\text{HCO}^+(J=1\rightarrow 0)$ emission, which was observed towards the Cloverleaf quasar ($z = 2.56$) with the Very Large Array (VLA)⁶. Due to its strong gravitational magnification (magnification factor $\mu_L = 11$, Venturini & Solomon 2003), the Cloverleaf is the brightest CO source at high redshift, and it also exhibits bright $\text{HCN}(J=1\rightarrow 0)$ emission (Solomon et al. 2003) and emission from both C I fine structure lines (Weiss et al. 2003, 2005). A previous search for $\text{HCO}^+(J=4\rightarrow 3)$ emission in this source has been unsuccessful, setting an upper limit of 14 mJy on the peak line flux density (Wilner et al. 1995). We use a standard concordance cosmology throughout, with $H_0 = 73 \text{ km s}^{-1} \text{ Mpc}^{-1}$, $\Omega_M = 0.24$, and $\Omega_\Lambda = 0.72$ (Spergel et al. 2003, 2006).

2. OBSERVATIONS

We observed the $\text{HCO}^+(J=1\rightarrow 0)$ transition line ($\nu_{\text{rest}} = 89.1885230 \text{ GHz}$) towards H1413+117 (the Cloverleaf quasar) using the VLA in D configuration between 2005 November 26 and 2006 January 13. At the target z of 2.55784, the line is redshifted to 25.068166 GHz (11.96 mm). The total integration time amounts to 25.5 h. Observations were performed in fast-switching mode using the nearby source 14160+13204 (distance to the Cloverleaf: 1.8°) for secondary amplitude and phase calibration. Observations were carried out under excellent weather conditions with 23 antennas. The phase stability in all runs was excellent (typically $<15^\circ$ rms for the longest baselines). For primary flux calibration, 3C286 was observed during each run.

Two 25 MHz wide intermediate frequency bands (IFs) with seven 3.125 MHz channels each were observed simultaneously in the so-called 'spectral line' mode centered at the $\text{HCO}^+(J=1\rightarrow 0)$ line frequency, leading to an effective bandwidth of 43.75 MHz (corresponding to 523 km s^{-1} at 25.1 GHz). In addition, two 50 MHz (corresponding to 598 km s^{-1} at 25.1 GHz) IFs were observed in the so-called 'quasi-continuum' mode at 24.7351 GHz and 24.7851 GHz to monitor the continuum at 12 mm. We chose a setting with both continuum channels below the $\text{HCO}^+(J=1\rightarrow 0)$ line frequency to avoid the significantly worse system temperatures and locking problems of the local oscillator (LO) above 25 GHz. The continuum was observed for one third of the total time to attain the same rms as in the combined line channels.

For data reduction and analysis, the *AIPS* package was used. The two continuum channels were concatenated in the uv/visibility plane. The $\text{HCO}^+(J=1\rightarrow 0)$ line data cube was generated by subtracting a CLEAN component model of the continuum emission from the visibility data. All data were mapped using the CLEAN algorithm and 'natural' weighting without applying a further taper; this results in a synthesized beam of $4.0'' \times 3.0''$ ($\sim 28 \text{ kpc}$ at $z = 2.56$). The final rms in the combined map is $16 \mu\text{Jy beam}^{-1}$ for a 34.375 MHz (corresponding to 411 km s^{-1}) channel, and $50 \mu\text{Jy beam}^{-1}$ for a 6.25 MHz (75 km s^{-1}) channel.

3. RESULTS

⁶ The Very Large Array is a facility of the National Radio Astronomy Observatory, operated by Associated Universities, Inc., under a cooperative agreement with the National Science Foundation.

We have detected emission from the $\text{HCO}^+(J=1\rightarrow 0)$ transition line towards the Cloverleaf quasar ($z = 2.56$). The source appears to be marginally resolved in both the continuum and the HCO^+ line maps. Two-dimensional Gaussian fitting yields a continuum peak flux density of $343 \pm 12 \mu\text{Jy beam}^{-1}$. The continuum-subtracted $\text{HCO}^+(J=1\rightarrow 0)$ line map is shown in Fig. 1. The cross indicates the geometrical center position of the resolved $^{12}\text{CO}(J=7\rightarrow 6)$ map at $\alpha = 14^\circ 15^m 46^s.233$, $\delta = +11^\circ 29' 43''.50$ (Alloin et al. 1997). The small offset is likely due to the fact that the lens images are not equally bright, i.e. the center of intensity is offset from the geometrical center position. The deconvolved source size from the Gaussian fit is in good agreement with the size of the resolved structure seen in $^{12}\text{CO}(J=7\rightarrow 6)$. The line is clearly detected at 8σ over a range of 34.375 MHz (411 km s^{-1}). We derive a line peak flux density of $193 \pm 28 \mu\text{Jy beam}^{-1}$. In Fig. 2, four channel maps (6.25 MHz, or 75 km s^{-1} each) of the central 25 MHz (300 km s^{-1}) of the $\text{HCO}^+(J=1\rightarrow 0)$ line are shown. At an rms of $50 \mu\text{Jy beam}^{-1}$, the line is detected at 4σ in the central two channels, and the decline of the line intensity towards the line wings is clearly visible in the outer channels, as expected. We attribute the small offset between the peak positions of channels 2 and 3 to observational uncertainties rather than to a real velocity gradient. We thus derive a $\text{HCO}^+(J=1\rightarrow 0)$ line luminosity of $L'_{\text{HCO}^+} = 3.5 \times 10^9 \text{ K km s}^{-1} \text{ pc}^2$ (corrected for gravitational magnification, $\mu_L = 11$, and the finite source size relative to the synthesized beam, which leads to a 30% correction based on the source extension seen in CO, see Table 1 and its caption for details).

We summarize our results in Table 1 together with the line fluxes and luminosities for HCN (Solomon et al. 2003) and CO (Weiss et al. 2003). Our $\text{HCO}^+(J=1\rightarrow 0)$ peak flux density corresponds to $\sim 80\%$ of the $\text{HCN}(J=1\rightarrow 0)$ peak flux of $0.24 \pm 0.04 \text{ mJy}$ derived by Solomon et al. (2003). This corresponds to a $L'_{\text{HCO}^+}/L'_{\text{HCN}}$ luminosity ratio of 0.8, which is consistent with unity within the statistical and systematical uncertainties. They use an extrapolated continuum peak flux at 24.9 GHz of $S_{\text{cont}}(24 \text{ GHz}) = 0.26 \pm 0.03 \text{ mJy}$. The difference to our value may be due to problems with their extrapolation or calibration errors. However, it is also possible that the continuum of the Cloverleaf is variable at 25 GHz.

4. DISCUSSION

In the following, we discuss relationships between the emission observed in HCO^+ and other molecules and the far-IR continuum for a sample of low- z spiral and starburst galaxies (Nguyen-Q-Rieu et al. 1992; Imanishi et al. 2004; Gao & Solomon 2004a), low- z (U)LIRGs (Graciá-Carpio et al. 2006; Imanishi et al. 2006), and the Cloverleaf (this work; Solomon et al. 2003; Weiss et al. 2003) as shown in Fig. 3. As only an upper limit exists for the $^{12}\text{CO}(J=1\rightarrow 0)$ line emission in the Cloverleaf (Tsuboi et al. 1999), we here assume that CO is fully thermalized up to the $3\rightarrow 2$ transition (i.e., $L'_{\text{CO}(1-0)} = L'_{\text{CO}(3-2)}$). We do not discuss effects of differential lensing, which could distort the intrinsic luminosity ratios, as models indicate similar sizes for molecular and dust emission in the Cloverleaf (Solomon et al. 2003).

Figure 3a: L'_{HCO^+} correlates closely with L_{FIR} ; a linear least squares fit (excluding the Cloverleaf) yields $\log(L_{\text{FIR}}) = (1.11 \pm 0.06) \times \log(L'_{\text{HCO}^+}) + 2.2$. For HCN, Gao & Solomon (2004a) find $\log(L_{\text{FIR}}) = 0.97 \times \log(L'_{\text{HCN}}) + 3.1$ based on a larger sample of local starburst and spiral galaxies. Both slopes are consistent with unity.

Figure 3b: L'_{HCO^+} also correlates closely with L'_{HCN} ; a linear least squares fit (again excluding the Cloverleaf) yields $\log(L'_{\text{HCN}}) = (0.94 \pm 0.06) \times \log(L'_{\text{HCO}^+}) + 0.6$. Panels **a** and **b** of Fig. 3 thus exemplify that HCO^+ traces dense molecular gas as well as HCN, and its close correlation with the far-IR continuum emission suggests that HCO^+ may also be used as a star formation indicator. It is remarkable how well the Cloverleaf agrees with the correlations found for local galaxies ranging over more than three orders of magnitude in far-IR luminosity.

Figure 3c: Based on data from Kohno et al. (2001) and Kohno (2005), Imanishi et al. (2006) argue that AGN-dominated galaxies have higher HCN/HCO⁺ and HCN/CO ratios than starburst-dominated galaxies. In this diagram, AGN-dominated galaxies thus fall on the upper right side, and starburst-dominated galaxies fall on the lower left side. For the local starburst/spiral sample, we have taken the $L'_{\text{HCN}}/L'_{\text{HCO}^+}$ ratios from Nguyen-Q-Rieu et al. (1992) and the $L'_{\text{HCN}}/L'_{\text{CO}}$ ratios from Gao & Solomon (2004a). The Cloverleaf clearly falls on the lower left side of the diagram, putting it in the region of 'starburst-dominated' galaxies. Indeed, by decomposition of the dust spectrum into a warm (115 K) and a cooler (50 K) component, Weiss et al. (2003) find that about 60% of the dust emission emerges from the cooler component, which may well be dominated by heating from star formation. However, based on an Arp 220 template, Solomon et al. (2003) have shown that only about 20% of the total far-IR luminosity is powered by the starburst. It is therefore unclear whether or not this diagram should indeed be used to constrain the properties of high- z quasars.

Figure 3d: Based on their recent study of local (U)LIRGs, Graciá-Carpio et al. (2006) suggest that the $L'_{\text{HCN}}/L'_{\text{HCO}^+}$ ratio correlates with L_{FIR} ; their results indicate that HCN may not be an unbiased tracer of star formation. We show this relation including their sample together with the spiral/starburst sample described above and the Cloverleaf. We find no evidence for any correlation between $L'_{\text{HCN}}/L'_{\text{HCO}^+}$ and L_{FIR} over the increased luminosity and redshift range. We note that if the relation suggested by Graciá-Carpio et al. (2006) were to hold, we would not have been able to detect the $\text{HCO}^+(J=1 \rightarrow 0)$ line in the Cloverleaf, as $L'_{\text{HCN}}/L'_{\text{HCO}^+}$ would be ~ 3 .

As discussed above, the $L'_{\text{HCN}}/L'_{\text{HCO}^+}$ ratio is consistent with unity over a large range in far-IR luminosities. Together with multi-transition studies of both molecules available for some of the local galaxies (e.g. Seaquist & Frayer 2000), this result suggests that HCO^+ does not require special conditions to be excited. Also, it indicates that HCO^+ and HCN trace physically similar regions. Although being consistent with unity within the error bars, the ratio of HCN and HCO^+ luminosities may be larger than 1 in the Cloverleaf, and several mechanisms to explain such a difference have been discussed in

the literature. It has been argued that HCN emission in molecular clouds can be enhanced by mid-IR pumping of a 14 μm vibrational band (Aalto et al. 1995), but HCO^+ can be mid-IR-pumped under very similar conditions via a 12 μm vibrational band (Graciá-Carpio et al. 2006). Also, Gao & Solomon (2004a) have found that this mechanism does not appear to play a major role (their Fig. 5). It has also been suggested that the chemical abundance of HCN can be enhanced relative to CO and HCO^+ in the ambient X-ray radiation field of a strong AGN (Lepp & Dalgarno 1996). It is also possible that the HCO^+ abundance is decreased due to the ionizing field produced by cosmic rays (Seaquist & Frayer 2000): Cosmic rays ionize H₂, leading to the production of H₃⁺, which reacts with CO to form HCO^+ . The abundance of HCO^+ is thus affected by ratio of cosmic-ray ionization rate and gas density. While a higher ionizing flux favours the production of HCO^+ , it also increases the number of free electrons, which leads to a higher probability for recombination: At a gas density of $3 \times 10^4 \text{ cm}^{-3}$, an ionizing field comparable to that of the Galaxy may already be strong enough to significantly decrease the abundance of HCO^+ due to dissociative recombination of H₃⁺ (e.g. Phillips & Lazio 1995), and the ionizing field in the Cloverleaf is probably much stronger than the Galactic one.

Our finding that the HCN-to- HCO^+ luminosity ratio in the Cloverleaf is close to unity implies that the processes discussed here likely do not play a dominant role. All these chemical arguments, assume that the HCN and $\text{HCO}^+ J = 1 \rightarrow 0$ opacities are low and that the observed line intensities scale with the underlying molecular abundances. Observations of the ¹³C baring isotophemes of HCO^+ and HCN in nearby starburst galaxies have shown that the $\text{HCO}^+/\text{H}^{13}\text{CO}^+$ and $\text{HCN}/\text{H}^{13}\text{CN}$ ratios are similar to those seen in CO/¹³CO (Nguyen-Q-Rieu et al. 1992; Wang et al. 2004). From this it has been concluded that that the HCO^+ and HCN opacities are similar to those in CO with $\tau \simeq 3 - 4$ (see also Henkel et al. 1993), i.e. the emission is optically thick. This would imply that $L'_{\text{HCN}}/L'_{\text{HCO}^+}$ is solely determined by the relative area filling factors and excitation temperatures of both molecules. As the $\text{HCO}^+(J=1 \rightarrow 0)$ and $\text{HCN}(J=1 \rightarrow 0)$ excitation is likely to be close to thermalized for densities of $n(\text{H}_2) \gtrsim 10^5 \text{ cm}^{-3}$, this would naturally explain $L'_{\text{HCN}}/L'_{\text{HCO}^+} \simeq 1$ assuming that both molecules trace regions of similar density (i.e., similar volume). We conclude that HCO^+ compares favourably with HCN in terms of being a good tracer for dense molecular gas even in FIR-bright objects at high redshift.

The National Radio Astronomy Observatory is operated by Associated Universities Inc., under cooperative agreement with the National Science Foundation. D. R. acknowledges support from the Deutsche Forschungsgemeinschaft (DFG) Priority Programme 1177. C. C. acknowledges support from the Max-Planck-Gesellschaft and the Alexander von Humboldt-Stiftung through the Max-Planck-Forschungspreis. The authors would like to thank the referee for useful comments which helped to improve the manuscript.

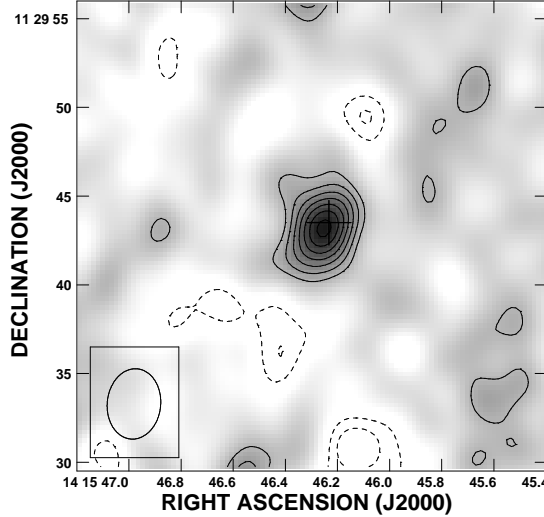


FIG. 1.— VLA detection of $\text{HCO}^+(J=1\rightarrow 0)$ towards the Cloverleaf quasar at a resolution of $4.0''\times 3.0''$ (as indicated in the bottom left corner). Continuum emission was subtracted. The source is marginally resolved. The cross indicates the geometrical center of the CO emission in the Cloverleaf (Alloin et al. 1997, see text). This continuum-subtracted map is integrated over the central 411 km s^{-1} (34.375 MHz). Contours are shown at $(-3, -2, 2, 3, 4, 5, 6, 7, 8)\times\sigma$ ($1\sigma = 16 \mu\text{Jy beam}^{-1}$).

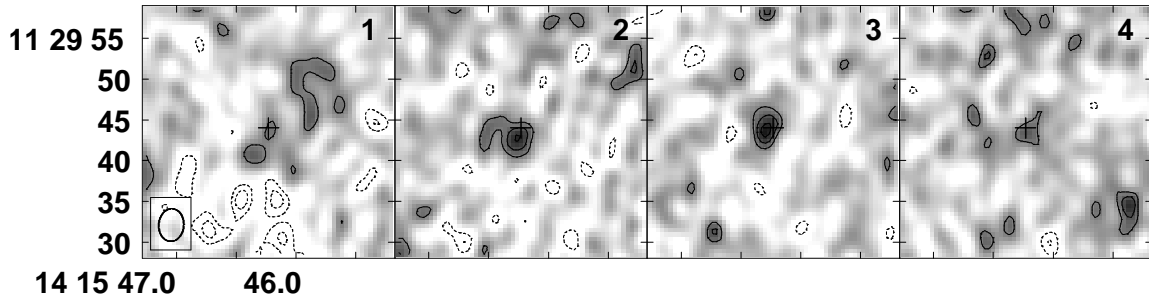


FIG. 2.— Channel maps of the $\text{HCO}^+(J=1\rightarrow 0)$ emission (same region is shown as in Fig. 1). One channel width is 6.25 MHz , or 75 km s^{-1} (frequencies increase with channel number and are shown at $25057.228, 25063.478, 25069.728$ and 25075.978 MHz). Contours are shown at $(-3, -2, 2, 3, 4)\times\sigma$ ($1\sigma = 50 \mu\text{Jy beam}^{-1}$). The beam size ($4.0''\times 3.0''$) is shown in the bottom left corner; the cross indicates the same position as in Fig. 1.

REFERENCES

Aalto, S., Booth, R. S., Black, J. H., & Johansson, L. E. B. 1995, *A&A*, 300, 369
 Alloin, D., Guilloteau, S., Barvainis, R., Antonucci, R., & Tacconi, L., 1997, *A&A*, 321, 24
 Brouillet, N., Muller, S., Herpin, F., et al. 2005, *A&A*, 429, 153
 Carilli, C. L., Solomon, P. M., Vanden Bout, P. A., et al. 2005, *ApJ*, 618, 586
 Gao, Y., & Solomon, P. M. 2004a, *ApJS*, 152, 63
 Gao, Y., & Solomon, P. M. 2004b, *ApJ*, 606, 271
 Graciá-Carpio, J., García-Burillo, S., Planesas, P., & Colina, L. 2006, *ApJ*, 640, L135
 Henkel, C., Mauersberger, R., Wiklind, T., et al. 1993, *A&A*, 268, L17
 Imanishi, M., Nakanishi, K., Kuno, N., & Kohno, K. 2004, *AJ*, 128, 2037
 Imanishi, M., Nakanishi, K., & Kohno, K. 2006, *AJ*, in press
 Kohno, K., Matsushita, S., Vila-Vilaro, B., et al. 2001, *ASP Conf. Ser. 249: The Central kpc of Starbursts and AGN*, 672
 Kohno, K. 2005, *AIP Conf. Ser. 783: The Evolution of Starbursts*, 203
 Lepp, S., & Dalgarno, A. 1996, *A&A*, 306, L21
 Nguyen-Q-Rieu, Jackson, J. M., Henkel, C., Truong-Bach, & Mauersberger, R. 1992, *ApJ*, 399, 521
 Phillips, J. A., & Lazio, T. J. W. 1995, *ApJ*, 442, L37
 Seaquist, E. R., & Frayer, D. T. 2000, *ApJ*, 540, 765
 Solomon, P., Downes, D., & Radford, S. 1992a, *ApJ*, 387, L55
 Solomon, P. M., Radford, S. J. E., & Downes, D. 1992b, *Nature*, 356, 318
 Solomon, P., Vanden Bout, P., Carilli, C., & Guelin, M. 2003, *Nature* 426, 636
 Solomon, P., & Vanden Bout, P. A. 2005, *ARA&A*, 43, 677
 Spergel, D. N., Verde, L., Peiris, H. V., et al. 2003, *ApJS*, 148, 175
 Spergel, D. N., Bean, R., Doré, O., et al. 2006, *ApJ*, submitted
 Tsuboi, M., Miyazaki, A., Imaizumi, S., & Nakai, N. 1999, *PASJ*, 51, 479
 Usero, A., García-Burillo, S., Fuente, A., et al. 2004, *A&A*, 419, 897
 Vanden Bout, P., Solomon, P., & Maddalena, R. 2004, *ApJ*, 614, L97
 Venturini, S., & Solomon, P. M. 2003, *ApJ*, 590, 740
 Wagg, J., Wilner, D. J., Neri, R., Downes, D., & Wiklind, T. 2005, *ApJ*, 634, L13
 Wang, M., Henkel, C., Chin, Y.-N., et al. 2004, *A&A*, 422, 883
 Weiß, A., Henkel, C., Downes, D., & Walter, F. 2003, *A&A*, 409, L41
 Weiß, A., Downes, D., Henkel, C., & Walter, F. 2005, *A&A*, 429, L25
 Wilner, D. J., Zhao, J.-H., & Ho, P. T. P. 1995, *ApJ*, 453, L91

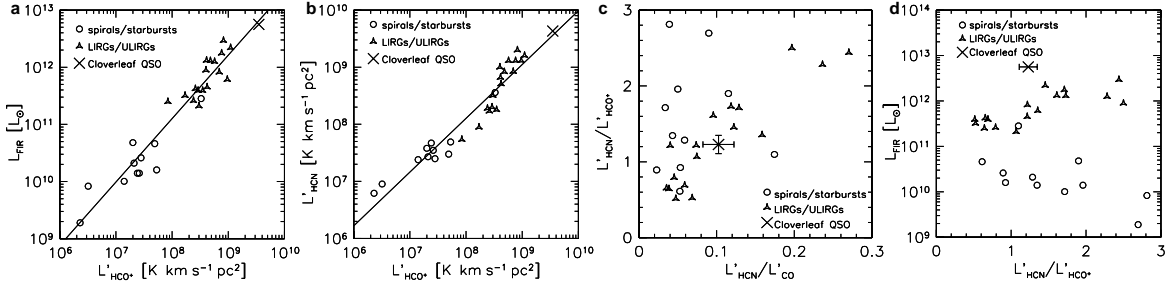


FIG. 3.— HCO⁺ luminosity relations for a sample of low- z spiral and starburst galaxies (Nguyen-Q-Rieu et al. 1992; Imanishi et al. 2004; Gao & Solomon 2004a), low- z (U)LIRGs (Graciá-Carpio et al. 2006; Imanishi et al. 2006), and the Cloverleaf (this work; Solomon et al. 2003; Weiss et al. 2003). The Cloverleaf luminosities are corrected for gravitational lensing ($\mu_L = 11$). The solid lines are least squares fits to all data except the Cloverleaf. The error bars shown for the Cloverleaf indicate the statistical errors of the line luminosity measurements. See text for more details.

TABLE 1
CO, HCN, AND HCO⁺ LINE LUMINOSITIES IN THE
CLOVERLEAF.

	S_ν [μ Jy]	L' [10^9 K km s ⁻¹ pc ²]	Ref.
HCO ^{+(J=1\rightarrow 0)}	193 ± 28	3.5 ± 0.3	1
HCN($J=1\rightarrow 0$)	240 ± 40	4.3 ± 0.5	2
¹² CO($J=3\rightarrow 2$)	30000 ± 1700	42 ± 7	3

REFERENCES. — [1] This work, [2] Solomon et al. (2003), [3] Weiss et al. (2003).

NOTE. — Luminosities are derived as described by Solomon et al. (1992b): $L'[\text{K km s}^{-1}\text{pc}^2] = 3.25 \times 10^7 \times I \times \nu_{\text{obs}}^{-2} \times D_L^2 \times (1+z)^{-3}$, where I is the velocity-integrated line flux in Jy km s⁻¹, D_L is the luminosity distance in Mpc ($z = 2.55784$, Weiss et al. 2003), and ν_{obs} is the observed frequency in GHz. All given luminosities are corrected for this lensing magnification. The HCN and HCO⁺ luminosities are corrected for the finite source size relative to the synthesized VLA beam (see text).